

Supporting Information:

Layered Phosphonates in Colloidal Synthesis of Anisotropic ZnO Nanocrystals

Bryan M. Tienes, Russell J. Perkins, Richard K. Shoemaker, Gordana Dukovic*

Department of Chemistry and Biochemistry, University of Colorado Boulder, Boulder, CO 80304

*To whom correspondence should be addressed.

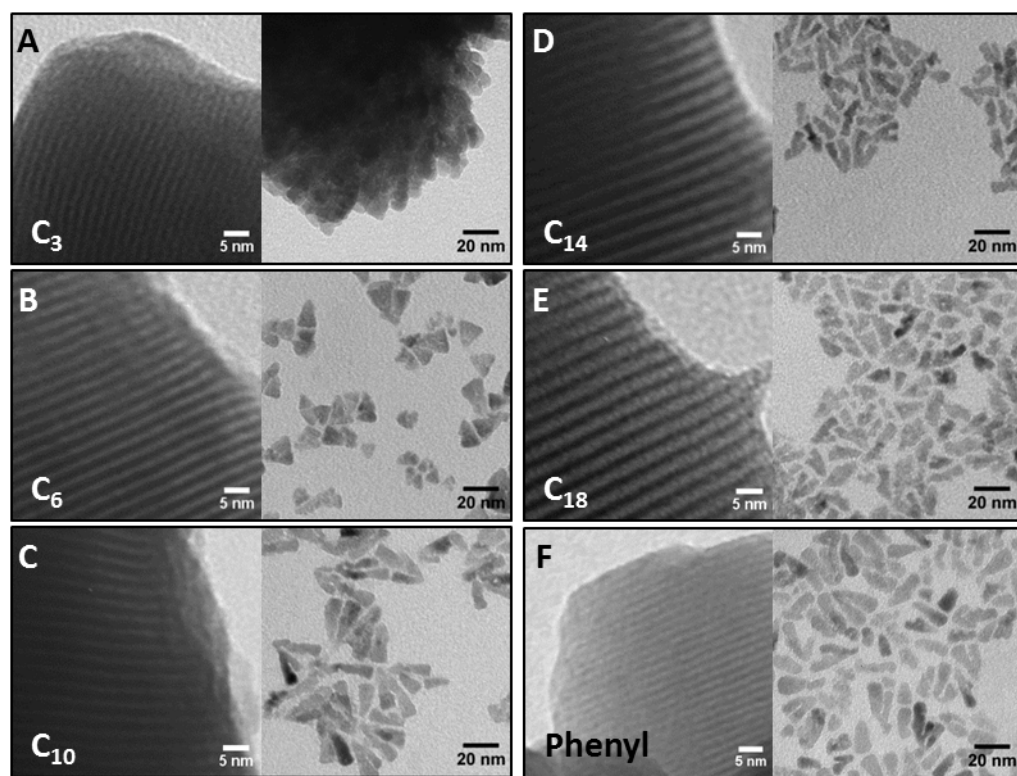


Figure S1. The left panel of each set (A-F) of images contains a TEM image of the layered phosphonate that was isolated as the intermediate in ZnO nanocrystal synthesis from $\text{Zn}(\text{OAc})_2$ and phosphonic acid precursors. The right panel of each set (A-F) contains a TEM image of the nanocrystals that were prepared in the continued reaction of the Zn-PA precursor and residual $\text{Zn}(\text{OAc})_2$ with 1-undecanol. The PAs associated with each set: (A) Propyl (C₃) phosphonic acid, (B) Hexyl (C₆) phosphonic acid, (C) Decyl (C₁₀) phosphonic acid, (D) Tetradecyl (C₁₄) phosphonic acid, (E) Octadecyl (C₁₈) phosphonic acid, and (F) Phenyl phosphonic acid

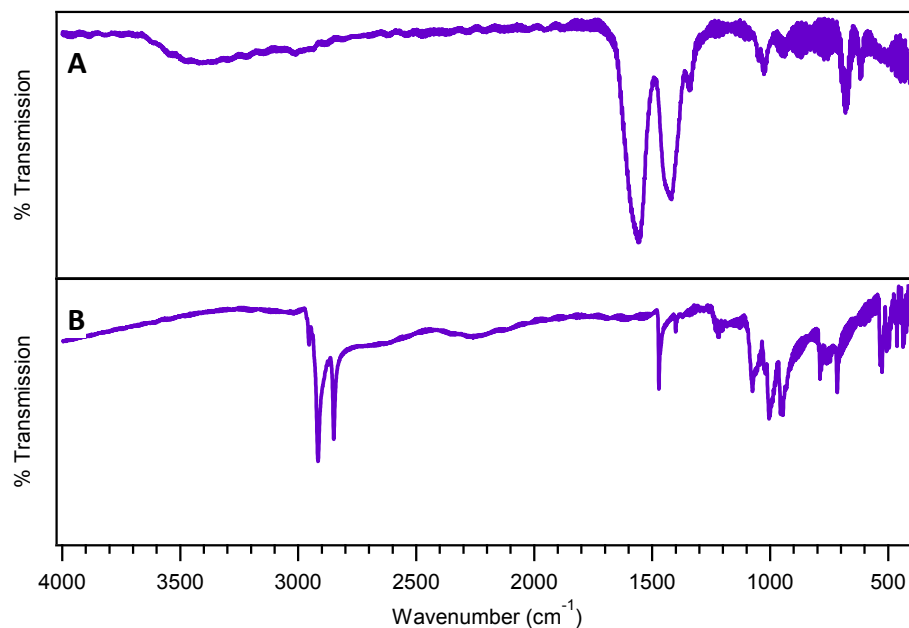


Figure S2. FTIR of solid starting materials in ZnO nanorod synthesis: (A) $\text{Zn}(\text{OAc})_2$. The spectrum contains strong C=O stretches at 1554 cm^{-1} and 1417 cm^{-1} (B) Octadecylphosphonic acid (ODPA). The spectrum contains C-H stretches between 3000 and 2800 cm^{-1} ; a C-H scissor mode peak at 1471 cm^{-1} ; and P-O peaks between 1250 and 900 cm^{-1} .

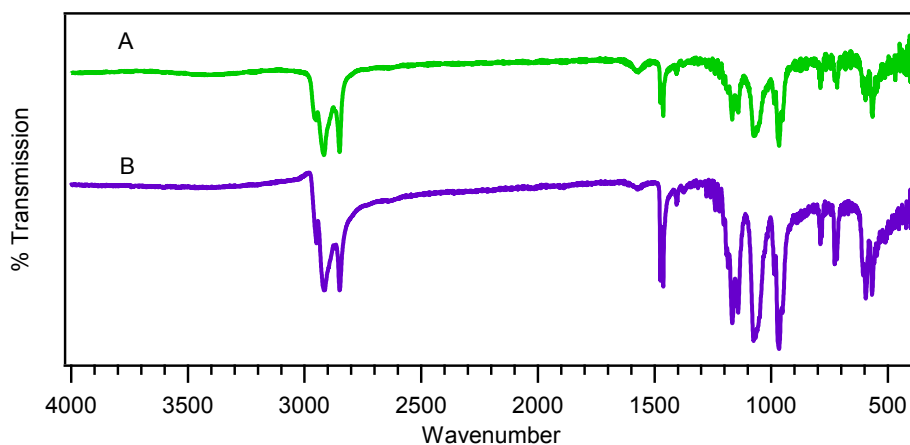


Figure S3. (A) FTIR spectrum of the insoluble intermediate formed during *ZnO nanorod* synthesis. (B) FTIR spectrum of the intermediate formed in the absence of trioctylphosphine oxide (TOPO). The spectra are offset for clarity. They contain identical features, indicating the absence of TOPO in the Zn-ODP structures.

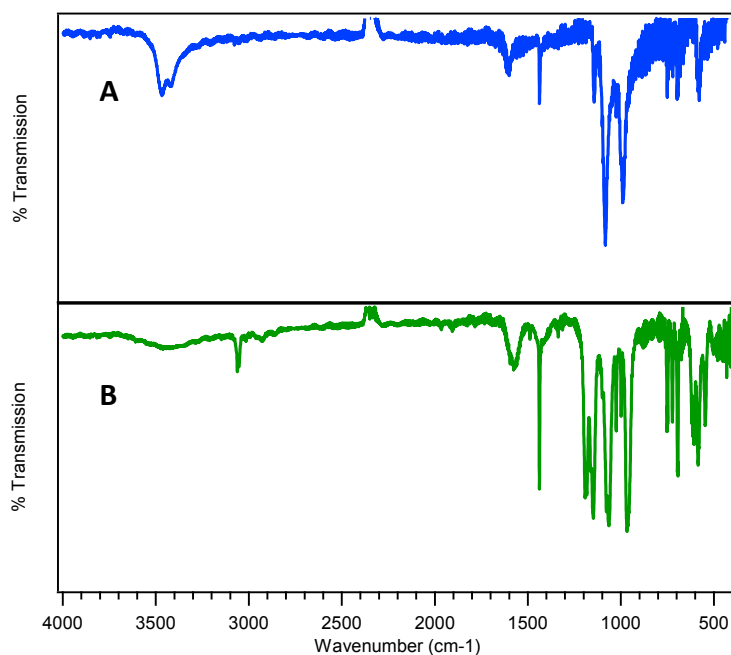


Figure S4. (A) FTIR of zinc phenylphosphonate made using an aqueous preparation (see Methods). (B) FTIR of the zinc phenylphosphonate made in the precursor formation step of ZnO nanorod synthesis using phenyl PA instead of ODPA. These spectra match the spectra reported by Clearfield et. al. for hydrated and dehydrated zinc phenylphosphonates.¹

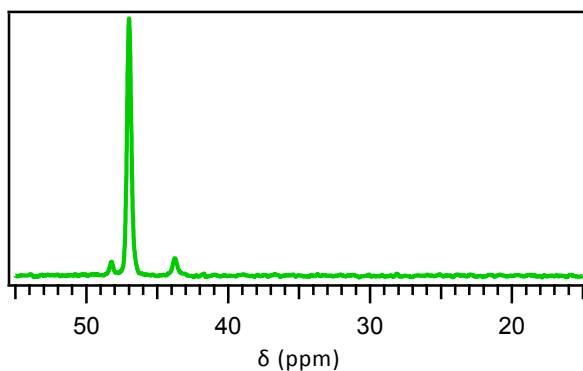


Figure S5. ^{31}P MAS (10 kHz) solid state NMR spectrum of TOPO. The chemical shift is substantially farther downfield than the peaks observed for ODPA or Zn-ODP in Figure 5A.

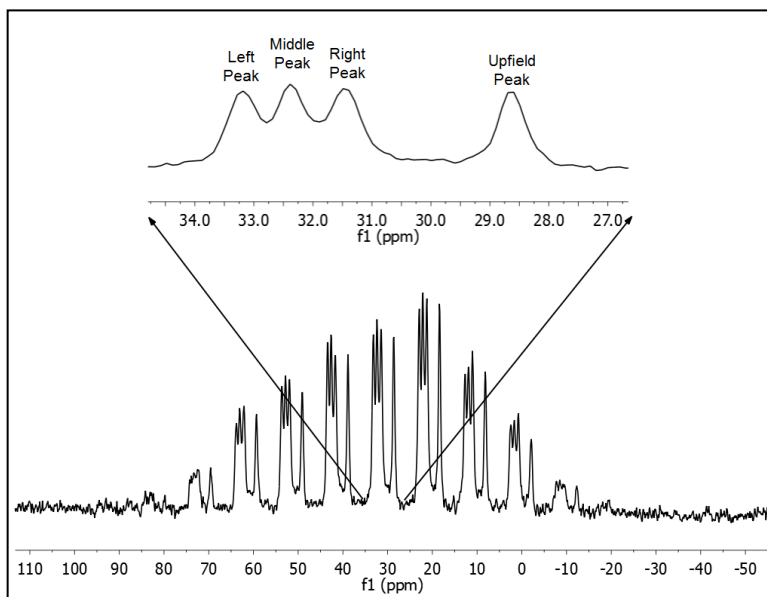


Figure S6. ^{31}P MAS NMR collected at 2kHz to determine the tensor parameter for each of the four peaks in the Zn-ODP spectrum. The isotropic peaks are expanded and labeled for clarity.

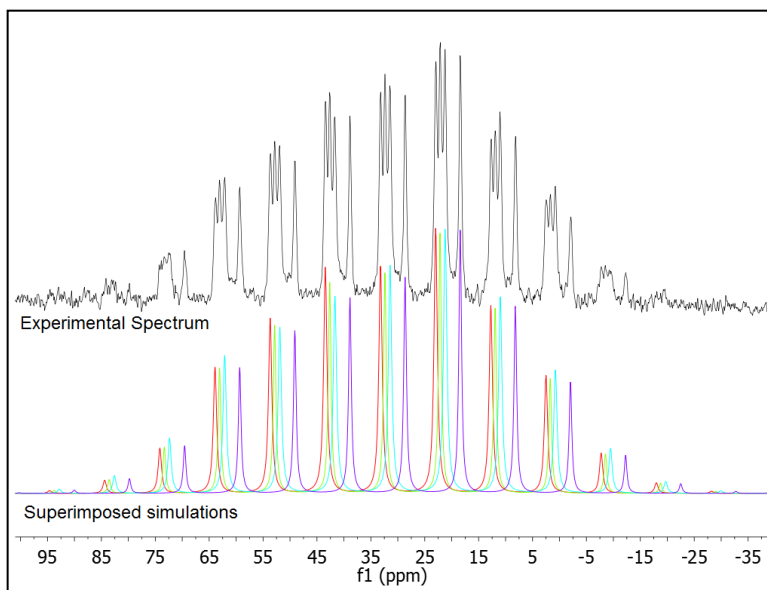


Figure S7. (top) The experimental MAS (2 kHz) ^{31}P NMR spectra of Zn-ODP. (bottom) Overlaid simulated spectra generated using the STARS simulation package in the VNMRJ 3.2A software (Agilent Technologies). The spectra of each of the four peaks were simulated independently of each other allowing the software to calculate a asymmetry parameter (η) and the chemical shift anisotropy (Δ) for each peak.

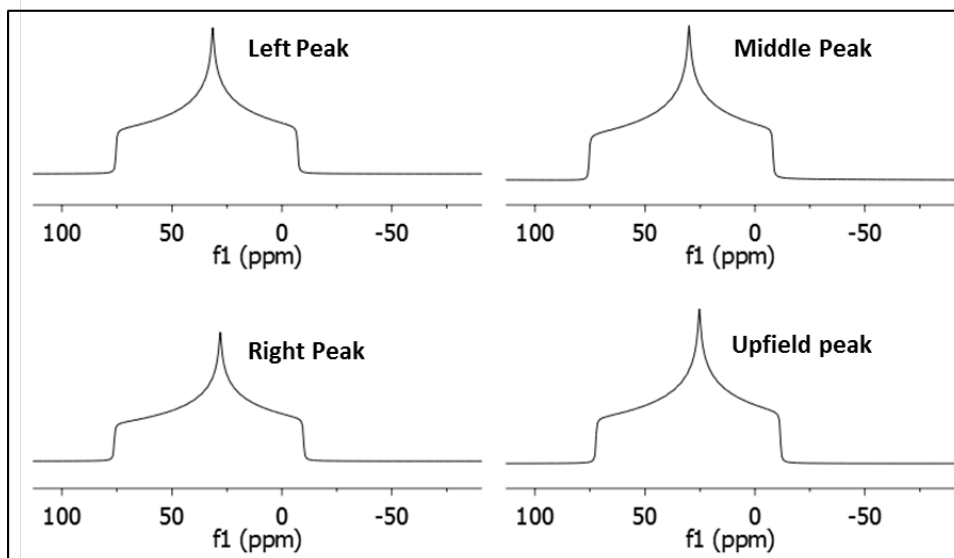


Figure S8. The simulated static solid ^{31}P NMR spectra for each of the four Zn-ODP peaks generated using the Agilent Technologies STARS software utility.

Table S1. Chemical shift tensor parameters for ODPA and Zn-ODP.

Sample	$\delta_{\text{iso}}^{\text{a}}$	δ_{zz}	δ_{yy}	δ_{xx}	η^{b}	Δ^{c}
ODPA	30.0	-16.45	45.82	60.53	0.28	-46.42
	28.7	72.35	25.24	-11.66	0.84	43.70
Zn-ODP	31.5	76.16	28.06	-9.83	0.85	44.70
	32.3	75.45	29.98	-8.28	0.89	43.06
	33.1	75.49	31.44	-7.31	0.92	42.28

a. δ_{iso} is the isotropic chemical shift and all values are relative to 85% H_3PO_4 ; $\delta_{\text{iso}} = (\delta_{\text{xx}} + \delta_{\text{yy}} + \delta_{\text{zz}})/3$

b. η is the asymmetry parameter; $\eta = (\delta_{\text{yy}} - \delta_{\text{xx}})/\Delta$;

c. Δ is the chemical shift anisotropy; $\Delta = \delta_{\text{zz}} - \delta_{\text{iso}}$

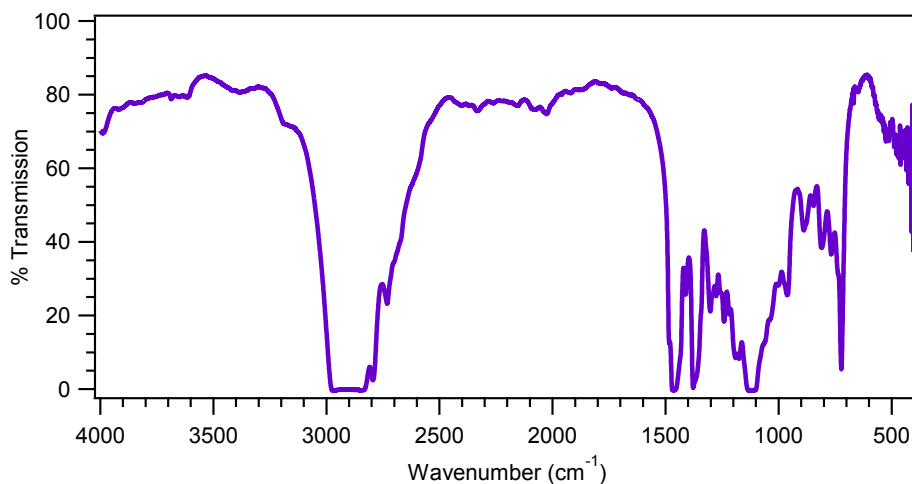


Figure S9. FTIR spectrum of octyl ether and TOPO (solvent mixture) using a 0.1 mm path length liquid FTIR cell. The solvents are in the same ratio as they are in the reaction. There is a window between 2500 cm^{-1} and 1500 cm^{-1} where the weak solvent absorption can be subtracted.

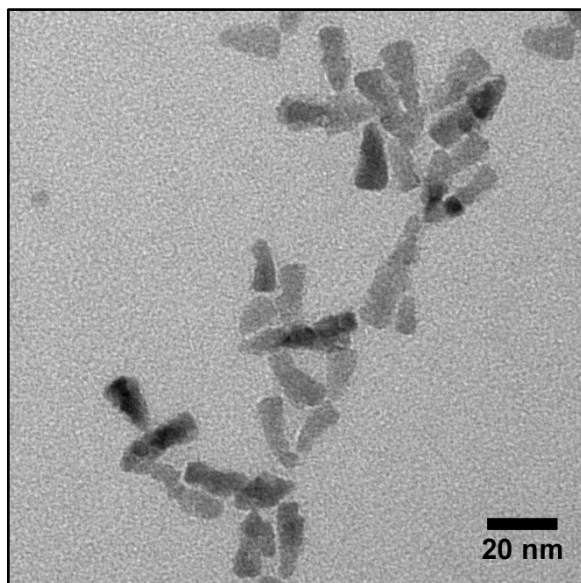


Figure S10. ZnO NRs synthesized using the procedure for ZnO nanorod synthesis (see Methods) with TOPO removed. [Reagent amounts: $\text{Zn}(\text{OAc})_2$ (1.0 mmol); ODPA (0.45 mmol); octyl ether (7.5 mL)]

Table S2. Size measurements of the nanocrystals formed as a result of the reaction of $\text{Zn}(\text{OAc})_2$ with 1-undecanol in the presence of phosphonic acids with different R groups. The number of particles measured for each PA, the length with one standard deviation, the width/base* with one standard deviation, and the aspect ratio from the average values are presented in the columns.

PA	# Measured	Length (nm)	Width (nm)*	Aspect ratio (l:w)
Hexyl (C6)	189	15 ± 5	11 ± 3	1.4 ± 0.6
Decyl (C10)	151	22 ± 5	7 ± 2	3.2 ± 1
Tetradecyl (C14)	155	18 ± 4	6 ± 1	3.0 ± 1
Octadecyl (C18)	338	18 ± 5	7 ± 2	2.5 ± 0.9
Phenyl	113	19 ± 5	7 ± 1	2.7 ± 0.9

*The width is defined as the base of the nanocone for the C6 case and the width at 50% of the length for the remaining PAs.

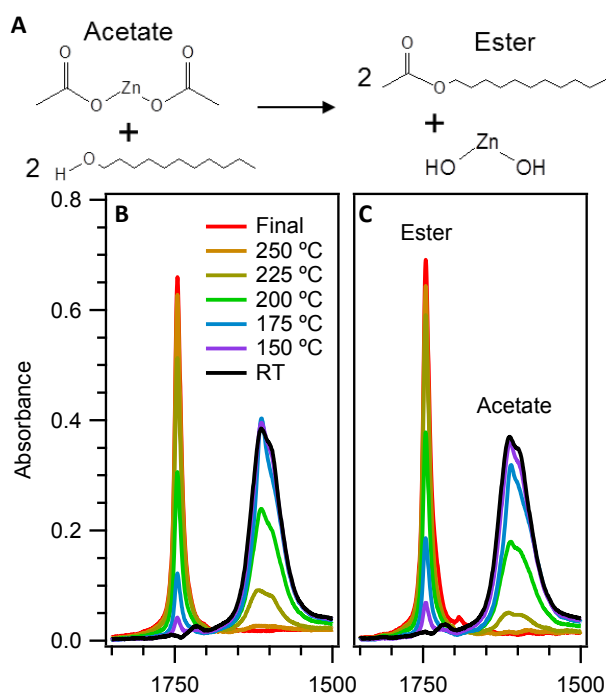


Figure S11. (A) Reaction scheme for the ester elimination that converts acetate into ester and $\text{Zn}(\text{OH})_2$. A comparison of the quantitative FTIR spectra (with solvent signal subtracted) during (B) the reaction lacking Zn-ODP (*Control A*) and (C) the *ZnO nanorod* synthesis. The aliquots are taken during the nanocrystal formation (i.e., after addition of 1-undecanol) when the reaction reaches the following points: (i) room temperature, (ii) 150 °C, (iii) 175 °C, (iv) 200 °C, (v) 225 °C, (vi) 250 °C, (vii) the crude final reaction mixture after 120 minutes at 250 °C. The broader peak around 1600 cm^{-1} is assigned to $\text{Zn}(\text{OAc})_2$ (Figure S2A), and the narrower peak near 1750 cm^{-1} corresponds to the carbonyl group of the ester formed when $\text{Zn}(\text{OAc})_2$ reacts with alcohol to form $\text{Zn}(\text{OH})_2$ ^{2, 3}. The kinetics of $\text{Zn}(\text{OAc})_2$ reaction with 1-undecanol are qualitatively similar in the presence of Zn-ODP. This similarity indicates that the production of $\text{Zn}(\text{OH})_2$ from $\text{Zn}(\text{OAc})_2$ proceeds at the same rates with and without Zn-ODP, and suggests that the impact of the ODPA addition occurs after $\text{Zn}(\text{OH})_2$ is formed.

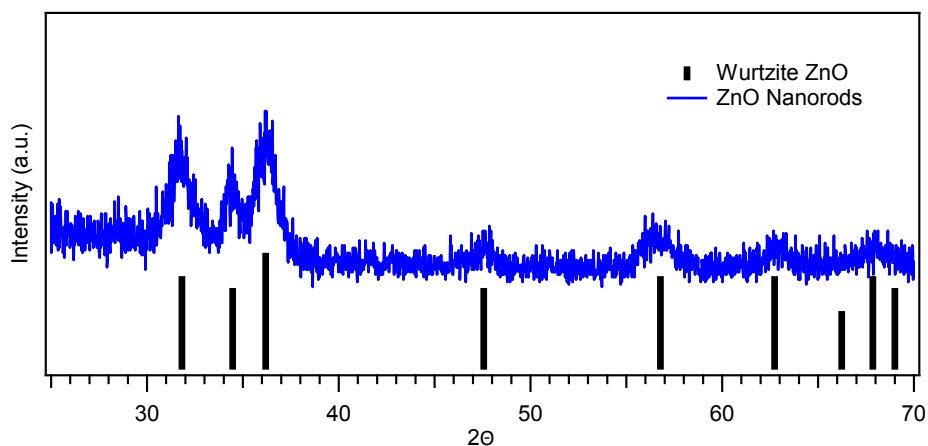


Figure S12. Powder XRD of ZnO nanorods (blue trace) and the wurtzite ZnO reference (black lines), indicating the nanorods are wurtzite ZnO.

References:

1. Frink, K. J.; Wang, R. C.; Colon, J. L.; Clearfield, A., Intercalation of Ammonia Into Zinc and Cobalt Phenylphosphonates. *Inorg. Chem.* 1991, 30, 1438-1441.
2. Joo, J.; Kwon, S. G.; Yu, J. H.; Hyeon, T., Synthesis of ZnO nanocrystals with cone, hexagonal cone, and rod shapes via non-hydrolytic ester elimination sol-gel reactions. *Adv. Mater. (Weinheim, Ger.)* 2005, 17, 1873-1877.
3. Kwon, S. G.; Hyeon, T., Colloidal Chemical Synthesis and Formation Kinetics of Uniformly Sized Nanocrystals of Metals, Oxides, and Chalcogenides. *Acc. Chem. Res.* 2008, 41, 1696-1709.